

# FE modeling of FRP strengthened CHS members subjected to lateral impact

M.I. Alam, S. Fawzia & Tafsirojjaman

*School of Civil Engineering and Built Environment, Science and Engineering Faculty, Queensland University of Technology (QUT), 2 George Street, Brisbane, QLD 4000, Australia*

X.-L. Zhao

*Department of Civil Engineering, Monash University, Melbourne, VIC 3800, Australia*

**ABSTRACT:** This paper presents the detailed finite element (FE) numerical modeling technique and dynamic lateral impact simulation of bare and FRP strengthened circular hollow section (CHS) tubular members. The equivalent composite layer technique is adopted to simulate experimental failure characterizes of FRP laminates and strengthened members. The FE analysis results are compared with the drop hammer lateral impact test results. Very good agreement between the lateral displacement-time curves of bare and strengthened specimens is observed. Both local and global deformation failures of the specimens are well predicted from dynamic impact simulation. Moreover, FE analysis results confirm that the FRP debonding failure at the impact location of the specimens can be simulated with reasonable accuracy. Thus, the current numerical analysis technique can be adopted to accurately predict the lateral impact responses of FRP strengthened hollow tubular members.

## 1 INTRODUCTION

The superior properties of tubular shape hollow steel members have been well recognized in the field of structural engineering for a long time. The better performance of these types of structures against bending, torsion and compression as well as architectural beauty, always put them in the top priority list in the construction industry. Hollow structural members often experience dynamic transverse impact loads from moving vehicles, heavily loaded ships, explosive attacks or from flying debris when they are used in multi-storey car parks, bridge piers, overpass bridges, building columns, utility poles, offshore structures. Significant damage or failure of these critical infrastructures can be expected if they are not designed to withstand lateral impact force.

In recent years, fibre reinforced polymer (FRP) strengthening of steel structural members has gained wide acceptance among the structural engineering research community due to several advantages of such method over the conventional strengthening/retrofitting method. A significant amount of experimental studies have been conducted over the last decade to understand the performance of FRP strengthened steel plates and members subjected to different loading conditions (Fawzia et al. 2010; Fawzia 2013; Kabir et al. 2016; Alam et al. 2014; Alam et al. 2017a; Alam et al. 2017b). However, compared to experimental works, finite element (FE) numerical studies of FRP strengthened steel structures are limited in the literature. Very recently, FE

numerical models of FRP strengthened square hollow section and concrete filled circular hollow section tubular steel columns were developed and transverse impact analysis were conducted to investigate the effect of FRP strengthening (Alam and Fawzia 2015; Alam et al. 2015; Alam et al. 2016). However, there is a lack of knowledge of dynamic FE analysis of FRP strengthened circular hollow section (CHS) tubular members subjected to lateral impact.

In this study, three-dimensional (3-D) FE models of FRP strengthened CHS tubular members are developed and dynamic transverse impact simulation was performed using ABAQUS/Explicit (SIMULIA 2011). The impact analysis results and the failure modes of the FE models are compared with the experimental tests conducted by the authors group. The predicted FE results and failure behavior of bare and strengthened members have shown good agreement with the test results.

## 2 EXPERIMENTAL TESTS

Laboratory drop mass lateral impact tests of bare and FRP strengthened CHS members were conducted (Alam et al. 2017a). All the CHS steel test specimens were fabricated from 6500 mm length steel pipe in identical dimensions of 1600 mm of length, 114.5 mm of outer diameter and 4.5 mm wall thickness. The test specimens were strengthened by externally bonded FRP sheets. The different FRP

types: carbon fibre reinforced polymer (CFRP) and glass fibre reinforced polymer (GFRP) were used for strengthening purpose. Two-part epoxy adhesive was used as bonding material. Lateral impact tests were performed at the mid-span of the specimens and the end conditions of the specimens were simply supported. The detail of specimen preparation and test setup can be found in elsewhere (Alam et al. 2017a). Figure 1 shows the schematic view of drop mass impact test setup. The detail of impact test matrix is listed in Table 1.

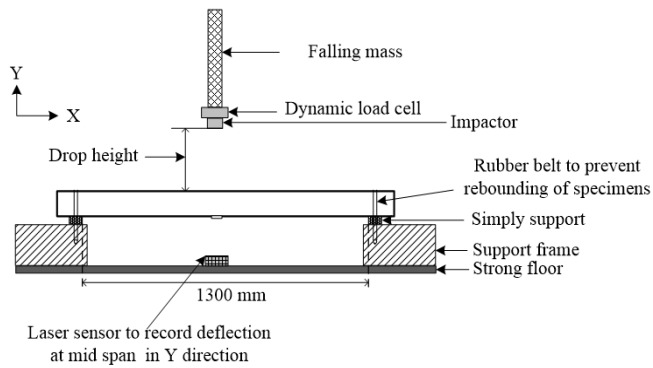


Figure 1. Experimental test setup (Alam et al. 2017a).

Table 1. Experimental test matrix.

Specimen ID	FRP layers	FRP type	Impact velocity (m/s)	FRP bond length (mm)
S-B-V1	-	-	3.28	-
C-L-V1	1	CFRP	3.28	1300
C-LL-V1	2	CFRP	3.60	1300
C-LL-V2	2	CFRP	3.28	1300
C-HL-V1	2	CFRP	3.28	1300
C-LLL-V1	3	CFRP	3.28	1300
C-LHL-V1	3	CFRP	3.28	1300
C-HLH-V1	3	CFRP	3.28	1300
G-LL-V1	2	GFRP	3.28	1300
G-HL-V1	2	GFRP	3.28	1300
GC-LL-V1	2	GFRP+CFRP	3.28	1300
C-LL975-V1	2	CFRP	3.28	975
C-LL650-V1	2	CFRP	3.28	650

### 3 FINITE ELEMENT MODELLING

#### 3.1 General

A total of 13 full length 3-D numerical models of bare and FRP strengthened CHS tubular members were developed using ABAQUS/Explicit (SIMULIA

2011). The dimension of the specimens was kept same as measured specimens dimension during experimental test. It was noticed that all one, two and three layers epoxy cured FRP sheets formed a single composite plate (Alam et al. 2017a). A thin adhesive layer also developed between the steel surface and cured FRP composite plate. An attempt was made to incorporate the similar behavior of FRP strengthened specimens in FE models. Thus, FE model of a FRP wrapped specimen consists of three parts: steel tube, thin adhesive layer and equivalent composite layer as shown in Figure 2. The equivalent thickness of one, two and three layers FRP plates were selected as 0.7 mm, 1.4 mm and 2.1 mm, respectively which were similar as measured from test specimens. The thickness of adhesive layer was considered as 0.1 mm.

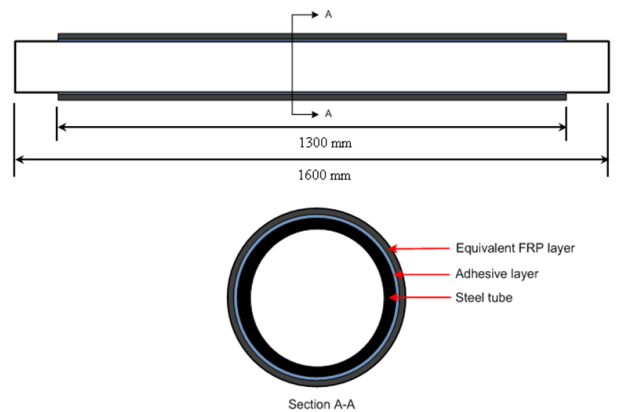


Figure 2. FE model of FRP strengthened CHS member.

In this work, the equivalent FRP plate was modeled using 8-node quadrilateral continuum shell element (SC8R). This element was also used in previous studies to model the FRP composite layers (Al-Zubaidy et al. 2012; Alam et al. 2015). The thin adhesive layer was modeled using 3-D cohesive element (COH3D8). Cohesive elements are capable of initiating debonding failure of FRP layers from steel surface. The thickness of adhesive layer was defined by the thickness of the cohesive element as 0.1 mm. The 8-node solid elements (C3D8R) were deployed to model CHS steel tubes. The drop mass impactor and the weight block were modeled using 8-node solid element. The dimension of the impactor head and the weight blocks were kept similar as experimental setup. The total mass of the drop mass unit was kept 592 kg by adjusting the densities of the weight block and impactor. Figure 3 depicts the FE model of FRP wrapped specimen subjected to lateral impact.

Comparatively dense meshing of elements was adopted at impact zone than the elements away from the impact zone to accurately capture the impact events. The 5 mm length elements were used to model impact zone whereas, 10 mm length element

was used to model the rest of the parts. The contact between the CHS steel tubes, adhesive and FRP layers were tied together using tie constrain available in ABAQUS library. The contact interactions between the impactor head and FRP layer, adhesive layer and outer surface of the steel tubes were simulated using general contact algorithm. The normal and tangential contact characteristics were defined by “Hard” contact, and “Penalty” friction formulation. The value of frictional coefficient was selected as 0.50 (Alam et al. 2017a; Alam et al. 2017b).

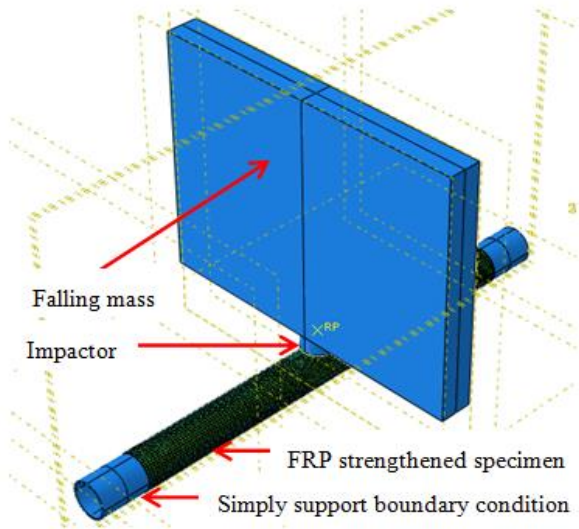


Figure 3 FE model of FRP strengthened CHS steel member subjected to transverse impact.

### 3.2 Material models

The failure behavior of FRP material was simulated using Hashin” failure criteria (Hashin 1980; Hashin and Rotem 1973). The static tensile coupon tests of CFRP and GFRP materials were conducted to obtain the mechanical properties used in this study. Table 2 presents the CFRP and GFRP tensile material properties obtained from coupon tests. The equivalent two and three layers FRP material properties were calculated using the equations proposed in early studies (Al-Zubaidy et al. 2012; Fawzia et al. 2006).

The cohesive elements were used to model the thin adhesive layer. The material failure behavior was defined by traction-separation law. The mechanical properties of epoxy adhesive were taken from coupon tests carried out by Kabir et al. (2016) (Table 3).

The material behavior of steel tubes was simulated using isotropic metal plasticity model. The materials properties listed in Table 2 were obtained from the tensile coupon tests extracted from tube samples.

The strain-rate effect was adopted by considering Cowper-Symonds power law relation.

Table 2. Material properties.

Properties	Steel	CFRP	GFRP	Adhesive
Elastic modulus (GPa)	211	75	23	3
Tensile Strength (MPa)	366	987	508	46
Yield Stress (MPa)	317	-	-	-

## 4 VALIDATION OF NUMERICAL MODELS

The initial impact velocity was applied to the falling mass and impactor to produce the same impact energies as recorded in impact tests at the mid-span of the specimens. Lateral impact simulations of all the test specimens were performed and the results were compared with the experimental tests. The numerical model validations were conducted by comparing the structural responses and failure modes of FE models and test specimens. Figure 4 displays the comparison of lateral displacement versus time responses of FE and test results. It can be seen that good agreements have found for bare steel, CFRP and GFRP wrapped members. Peak lateral displacements and average residual displacements between FE and tests displacement responses were well matched (Figure 4). Table 3 listed the comparison of peak lateral displacements between test and FE results. The predicted peak lateral displacements were closely matched with experimental test results with mean and COV were 1.02 and 0.03, respectively.

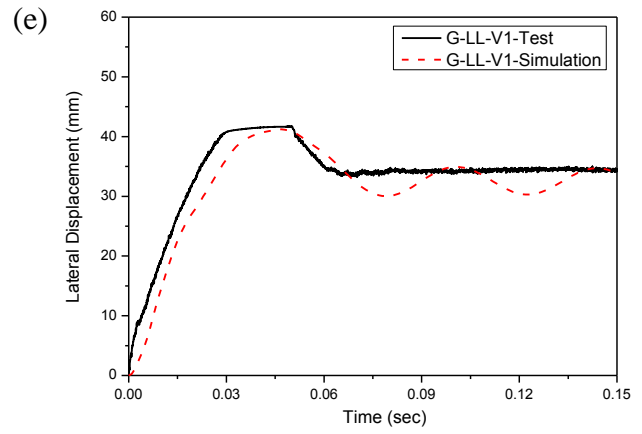
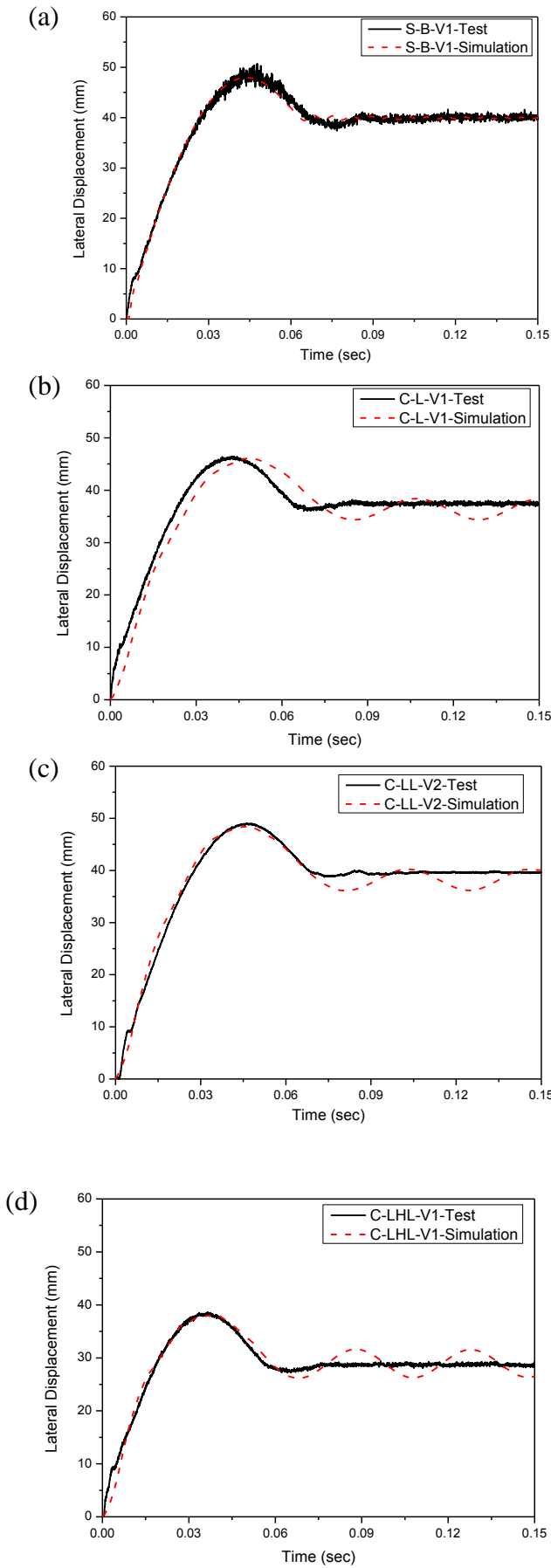


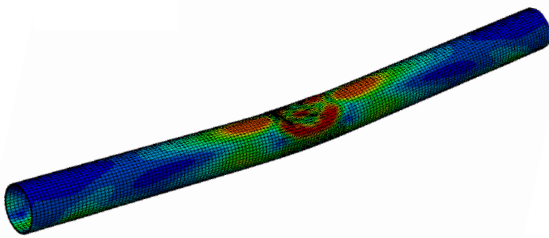
Figure 4. Comparison of Lateral displacement-time curves (a) bare, (b) one layer CFRP wrapped, (c) two layers CFRP wrapped, (d) three layers CFRP wrapped and (e) two layers GFRP wrapped steel tubes.

Table 3. FE and test results comparison.

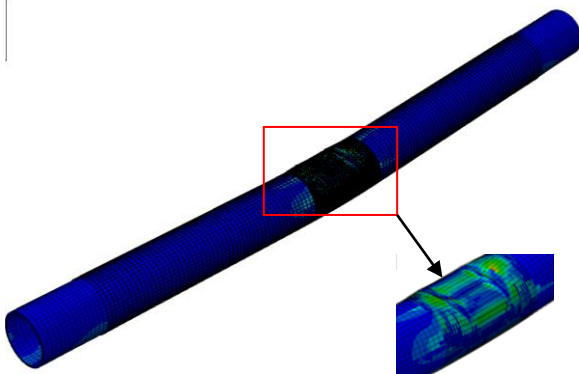
Specimen ID	$D_{p(test)}$ (mm)	$D_{r(FE)}$ (mm)	$D_{p(test)} / D_{r(FE)}$
S-B-V1	50.7	47.9	1.06
C-L-V1	46.5	46.0	1.01
C-LL-V1	39.1	39.6	0.99
C-LL-V2	49.0	47.9	1.02
C-HL-V1	39.4	37.1	1.06
C-LLL-V1	40.8	41.6	0.98
C-LHL-V1	38.6	38.1	1.01
C-HLH-V1	41.0	39.9	1.03
G-LL-V1	41.7	41.2	1.01
G-HL-V1	44.2	43.8	1.01
GC-LL-V1	45.1	43.3	1.04
C-LL975-V1	40.5	41.8	0.97
C-LL650-V1	43.3	41.7	1.04
Mean			1.02
COV			0.03

Note:  $D_{p(test)}$  = Peak lateral displacement;  $D_{r(FE)}$  = Average residual lateral displacement

The failure modes of bare and CFRP strengthened FE models were compared with the impacted specimens in Figure 5. The local and global deformation behaviors of test specimens were well predicted in FE models. The FRP fracture and debonding failure observed in test event were also predicted successfully in FE analysis. Moreover, no FRP debonding was noticed at both ends of the model. Similar failure behavior was also noticed in test specimen. Thus, the numerical modeling and dynamic impact analyses approach discussed in this work can be deployed to capture dynamic responses of bare and FRP wrapped CHS tubular members under transverse impact.



(a)



(b)

Figure 5. Failure mode comparison of (a) bare, (b) two layers CFRP strengthened CHS member.

## 5 CONCLUSIONS

In this study, FE numerical models of bare and FRP strengthened steel tubular members were developed and dynamic impact simulation was carried out to validate a series of impact test results. The findings and observations obtained from this research are outlined below:

1. 3-D full length FE models of bare and FRP wrapped steel tubular members were developed successfully to predict laboratory drop mass impact test responses of such structural members.
2. The dynamic impact simulation results have shown very good agreement of lateral displacement-time responses of bare and FRP strengthened specimens.
3. The failure modes of impact specimens were predicted by capturing both local and global deformation characteristics of bare and strengthened members with reasonable accuracy.
4. The obtained results confirmed that the current numerical technique can be implemented in future research to predict the behavior of FRP strengthened metallic structures subjected to transverse impact.

## REFERENCES

- Alam, M.I., Fawzia, S., & Batuwitige C. Dynamic simulation of CFRP strengthened steel column under impact loading. *In: proceedings of 23<sup>rd</sup> Australasian Conference on the Mechanics of Structures and Materials (ACMSM23), 9-12 December 2014*. Byron Bay: Australia.
- Alam, M.I., Fawzia, S., & Liu, X. 2015. Effect of bond length on the behaviour of CFRP strengthened concrete-filled steel tubes under transverse impact. *Composite Structures*, 132: 898-914.
- Alam, M.I., & Fawzia, S. 2015. Numerical studies on CFRP strengthened steel columns under transverse impact. *Composite Structures*, 120: 428-441.
- Alam, M.I., Fawzia, S., & Zhao, X.-L. 2016. Numerical investigation of CFRP strengthened full scale CFST columns subjected to vehicular impact. *Engineering Structures*, 126: 292-310.
- Alam M.I., Fawzia, S., Zhao, X.-L., & Remennikov, A.M. 2017. Experimental study on FRP strengthened steel tubular members under lateral impact. *Journal of Composites for Construction* 21(5): 1-14.
- Alam, M.I., Fawzia, S., Zhao, X.-L., Remennikov A.M., Bambach, M.R., & Elchalakani, M. 2017. Performance and dynamic behaviour of FRP strengthened CFST members subjected to lateral impact. *Engineering Structures*, 147: 160-176.
- Al-Zubaidy, H., Al-Mahaidi, R., @ Zhao, X.-L. 2012. Finite element modelling of CFRP/steel double strap joints subject-

- ed to dynamic tensile loadings. *Composite Structures* 99: 48-61.
- Bambach, M., Jama, H., Zhao, X., & Grzebieta, R. 2008. Hollow and concrete filled steel hollow sections under transverse impact loads. *Engineering Structures* 30: 2859–2870.
- Fawzia, S., Al-Mahaidi, R., and Zhao, X.-L. 2006. Experimental and finite element analysis of a double strap joint between steel plates and normal modulus CFRP. *Composite structures* 75(1): 156-162.
- Fawzia, S., Zhao, X.-L., & Al-Mahaidi, R. 2010. Bond-slip models for double strap joints strengthened by CFRP. *Composite Structures* 92(9): 2137–2145.
- Fawzia, S. 2013. Evaluation of shear stress and slip relationship of composite lap joints. *Composite Structures* 100: 548–553.
- Kabir, M.H., Fawzia, S., Chan, T.H.T., Gamage, J.C.P.H., & Bai, J.B. 2016. Experimental and numerical investigation of the behaviour of CFRP strengthened CHS beams subjected to bending. *Engineering Structures* 113: 160–173.
- Hashin, Z. 1980. Failure criteria for unidirectional fiber composites. *Journal of applied mechanics* 47(2): 329-334.
- Hashin, Z., & Rotem, A. 1973. A fatigue failure criterion for fiber reinforced materials. *Journal of composite materials* 7(4): 448-464.
- SIMULIA 2011. *ABAQUS analysis and theory manuals*, SIMULIA, the Dassault Systèmes, Realistic Simulation, Providence, RI, USA.
- Zeinoddini, M., Parke, G., & Harding, J. 2002. Axially pre-loaded steel tubes subjected to lateral impacts: an experimental study. *International Journal of Impact Engineering* 27: 669–90.